PROTOSTELLAR DISK FORMATION AND EARLY EVOLUTION

FRED C. ADAMS[1] AND GREGORY LAUGHLIN[2]

[1]*Department of Physics, University of Michigan, Ann Arbor, MI 48109*
[2]*NASA Ames Research Center, Moffett Field, CA 94720*

Abstract. This contribution describes the formation of circumstellar disks and their earliest evolutionary phases when self-gravity in the disk plays a crucial role in eliciting the transport of mass and angular momentum. We first discuss the formation of protostellar disks within the context of analytic infall-collapse solutions. We then discuss our efforts to understand the behavior of the newly formed disks. Our specific approach consists of performing a detailed analysis of a simplified model disk which is susceptible to the growth of a spiral instability. Using a combination of numerical simulation and semi-analytic analysis, we show how the dramatic early phase of mass and angular momentum transport in the disk can be explained by a second-order nonlinear process involving self-interaction of a dominant two-armed spiral mode.

Keywords: Self Gravitating Disks, Spiral Modes, Nonlinear Interactions

1. Introduction

The formation and early evolution of circumstellar disks is determined by the nature of the collapse flow that forms stars out of molecular cloud cores. In the current theory of star formation, molecular cloud cores provide the initial conditions for the star formation process. In particular, the process of star formation begins when these cores collapse. As the collapse proceeds, a pressure supported star forms at the center of the inward flow and a circumstellar disk forms around it from the infalling material with higher specific angular momentum (*cf.* the review of Shu *et al.*, 1987). During this early formative stage, a protostar thus consists of a central star/disk system which is deeply embedded within an infalling envelope of dust and gas. The characteristics of this infalling envelope largely determine the manner in which the protostar evolves and the nature of the circumstellar disk.

The first collapse calculations focused on isothermal cloud cores that are either perfectly spherical (Larson, 1969a; 1969b; Shu, 1977; Hunter, 1977) or slowly rotating (Cassen and Moosman, 1981; Terebey *et al.*, 1984). The resulting collapse solutions have been extremely useful in studies of low-mass protostars. In particular, these infall solutions have been used as a starting point for radiative transfer calculations to determine the spectral energy distributions of protostellar objects; the results are in good agreement with observed protostellar candidates (*e. g.*, Adams *et al.*, 1987; Butner *et al.*, 1991; Kenyon *et al.*, 1993).

These studies have shown that the collapse flow remains nearly spherical in the outer regions, *i. e.*, outside a centrifugal radius R_C which is determined by conservation of angular momentum. When magnetic fields are present, an analogous magnetic barrier occurs at the radius R_B where the Lorentz force of the

magnetic field exceeds that of gravity (see Galli and Shu, 1993ab). Disk formation is driven by the nature of the collapse solutions in the inner regime ($r \sim R_C$), where the infalling particles follow nearly ballistic trajectories as they spiral into the central star/disk system (Cassen and Moosman, 1981; Terebey *et al.*, 1984; see also Ulrich, 1976, and Chevalier, 1983). However, all of the early work in this regime was limited to the case of zero energy orbits and the gravitational potential of a point mass (namely the star).

In more recent work (Jijina and Adams, 1996), we have considered the additional effect of radiation pressure, which is important for protostellar objects with mass $M \geq 2\, M_{\odot}$. In the current star formation scenario, there is an "opacity gap" immediately surrounding the star; here, the dust evaporates and radiation streams freely through this region. At the dust evaporation radius (often denoted as the "dust destruction front"), the ultraviolet and visible photons are absorbed in a thin shell and the photons are thermalized. Outside this radius, the infalling envelope is optically thick at infrared wavelengths where the warm dust reradiates. The gradient of this infrared radiation provides a radiation pressure which acts to decelerate the infalling gas.

Radiation pressure has been considered previously for spherical collapse (Larson and Starrfield, 1971; Kahn, 1974; Wolfire and Cassinelli, 1986; 1987). These studies suggest that radiation pressure severely restricts the possible masses of forming stars. Nakano (1989) has argued that nonspherical infall can lead to the formation of more massive stars (see also Nakano *et al.*, 1995); this work assumes both a flattened density distribution and a nonspherical radiation field. In the study by Jijina and Adams (1996), we carry this idea further by finding a self-consistent infall-collapse solution which includes the effects of radiation pressure in the inner regime where rotation plays a large role and the flow is highly non-spherical. In this work, we assume a spherical radiation field and then calculate the corresponding nonspherical density field. The "inner" solutions resulting from this study can then be matched onto the "outer solutions" obtained elsewhere (*e. g.*, Shu, 1977) to provide a complete collapse solution for the star formation problem.

In any case, for the entire class of infall collapse solutions described above, the majority of the infalling mass falls directly onto the circumstellar disk, rather than directly onto the star. This result holds for virtually the whole regime of parameter space, with and without the effects of radiation pressure. For the standard collapse solution, the mass M_* that falls *directly* onto the star approaches a value that is asymptotically constant in time, *i. e.*, $M_* \to 1.293[16a^8 R_*/\Omega^2 G^3]^{1/3}$ (see Adams and Shu, 1986). As a reference point, for typical protostellar collapse parameters, this mass scale is about 0.05 $M_{\odot}$, much smaller than a typical star. If no disk accretion occurs, stars would be limited to this small mass scale, and the circumstellar disks would become much more massive than their central stars. Such a configuration is highly unstable, however, and must eventually lead to disk accretion, as we describe below.

2.   The Evolution of a Massive Protostellar Disk

The foregoing discussion has made it clear that gravitationally unstable disks must arise during the earliest phases of the star and planet formation process. Typical molecular cloud cores are in more or less rigid-body rotation, with masses on order 1–2 $M_{\odot}$, size 0.1 pc, and rotational frequencies $\Omega \sim 2 \times 10^{-14} \mathrm{s}^{-1}$ (Goodman *et al.*, 1993). The total angular momentum contained in a typical collapsing molecular cloud core is thus on order of $J \sim 1 \times 10^{54} \, \mathrm{g \, cm^2 \, s^{-1}}$. However, after timescales of roughly several 10^5 y, single protostar/protostellar disk systems are observed to have worked themselves down to total angular momenta on order $J \leq 10^{53} \, \mathrm{g \, cm^2 \, s^{-1}}$ (see, *e. g.*, the review article of Bodenheimer, 1995). The most straightforward interpretation of this discrepancy is that a very efficient angular momentum transport mechanism is operating during the earliest phases of protostellar disk evolution. Self-gravitating instabilities appear to be the best candidate for eliciting this rapid transport.

We will argue that the hydrodynamic processes occurring within massive protostellar disks are responsible for transporting angular momentum outwards while transporting mass inwards, and that these processes dictate the final outcome of the system, *i. e.* either a single star with planets or a multiple stellar system. In our picture, the saturation of spiral gravitational instabilities at a finite amplitude in a disk allows for the steady transport of mass and momentum, and eventually clears the way for a single star surrounded by planets (our own solar system being a typical example). In other cases, when the amount of angular momentum in the initial collapse flow is too great, then fragmentation of the collapsing cloud can occur, and binary or multiple star systems can form. Such dynamic formation of binaries is currently an active area of study (see *e. g.*, Burkert *et al.*, 1997).

The discussion which follows draws heavily from two of our recent papers (Laughlin *et al.*, 1997; 1998). The goal here is to give a self-contained description of the development of an unstable spiral mode. We hope that this approach can provide a familiarity with the behavior of the class of gravitational instabilities that are likely to occur in massive protostellar disks, and in particular we want to show how a combination of linear and nonlinear analyses, using both semi-analytical and numerical techniques, can give insight into the disk evolution and angular momentum transport processes.

Many authors have studied the evolution of self-gravitating protostellar disks with nonlinear simulations. This approach provides an immediate handle on the overall aspects of the problem. A useful selection of articles might include Heemskerk *et al.* (1992), Woodward *et al.* (1994), Tomley *et al.* (1994), Boss (1997), and Nelson *et al.* (1998).

As a specific example of this experimental/numerical approach, we will follow the complicated behavior of an idealized thin disk with the following properties: The disk's radial distribution of surface density has a Gaussian profile. The inner edge of the disk lies at $R_{\mathrm{in}} = 0.25$, and the outer edge of the disk lies at $R_{\mathrm{D}} = 1.0$,

while the radius R_0 at which the surface density peaks is taken to be $R_0 = 0.45$. The disk mass, m_D=0.4, is comparable to the central mass of $m_* = 0.6$ (note that G=1). The equation of state is polytropic with γ_p=2, and the polytropic constant is adjusted so that Q reaches a minimum value of Q=1.3 at r=0.5. Material is allowed to flow freely outward, but the inner boundary is reflective. This model, although idealized, is a very reasonable approximation to the kinds of disks that are expected to arise during the early phases of the collapse flow. Indeed, the disk model was inspired by direct radiation-hydrodynamical calculations of the collapse process (Yorke *et al.*, 1993; Laughlin and Bodenheimer, 1994).

The disk model is inserted into a finite difference code which solves the following equations of motion:

$$\frac{\partial u}{\partial t} + u\frac{\partial u}{\partial r} + \frac{v}{r}\frac{\partial u}{\partial \phi} - \frac{v^2}{r} = -\frac{\partial}{\partial r}\left(h + \Psi + \Psi_*\right), \tag{1}$$

$$\frac{\partial v}{\partial t} + u\frac{\partial v}{\partial r} + \frac{v}{r}\frac{\partial v}{\partial \phi} + \frac{vu}{r} = -\frac{1}{r}\frac{\partial}{\partial \phi}\left(h + \Psi + \Psi_*\right), \tag{2}$$

$$\frac{\partial \sigma}{\partial t} + \frac{1}{r}\frac{\partial}{\partial r}\left(r\sigma u\right) + \frac{1}{r}\frac{\partial}{\partial \phi}\left(\sigma v\right) = 0, \tag{3}$$

and

$$\Psi = -G\int_{R_{in}}^{R_D} \sigma(r', \phi')r'dr' \int_0^{2\pi} \frac{d\phi'}{\sqrt{r^2 + r'^2 - 2rr'\cos(\phi - \phi') + \epsilon^2(r)}}. \tag{4}$$

Most of the symbols have the same definitions as in Laughlin *et al.* (1998): u and v are the radial and azimuthal velocities within the disk, and σ is the surface density. The field Ψ is the gravitational potential, which includes an explicit contribution Ψ_* from the central star. The quantity ϵ appearing in the Poisson integral is a gravitational softening parameter, which is required in order to make the potential finite at the thin disk edges (see Appendix C of Laughlin *et al.*, 1998). All of the dependent variables are functions of the radius r, the azimuthal angle ϕ, and the time t. The pressure gradient of the disk material is expressed in terms of the enthalpy h.

Our hydrodynamics algorithm employs a second-order flux-conservative Van Leer type advection scheme to evolve the momentum and continuity equations in polar coordinates (for a description see Laughlin, 1994). The gravitational potential from the disk material is computed using a fast Fourier transform method as described in Binney and Tremaine (1987).

We use a system of units in which the initial outer radius of the disk, R_D, the total disk+star system mass, and the gravitational constant G are all equal to unity. A time of 1.0 thus corresponds to approximately one radian of angular revolution at the outer edge of the disk.

The simulation is launched by introducing a random perturbation of up to one part in 1000 to each of 256^2 grid cells, and the disk is released to follow the dictates of
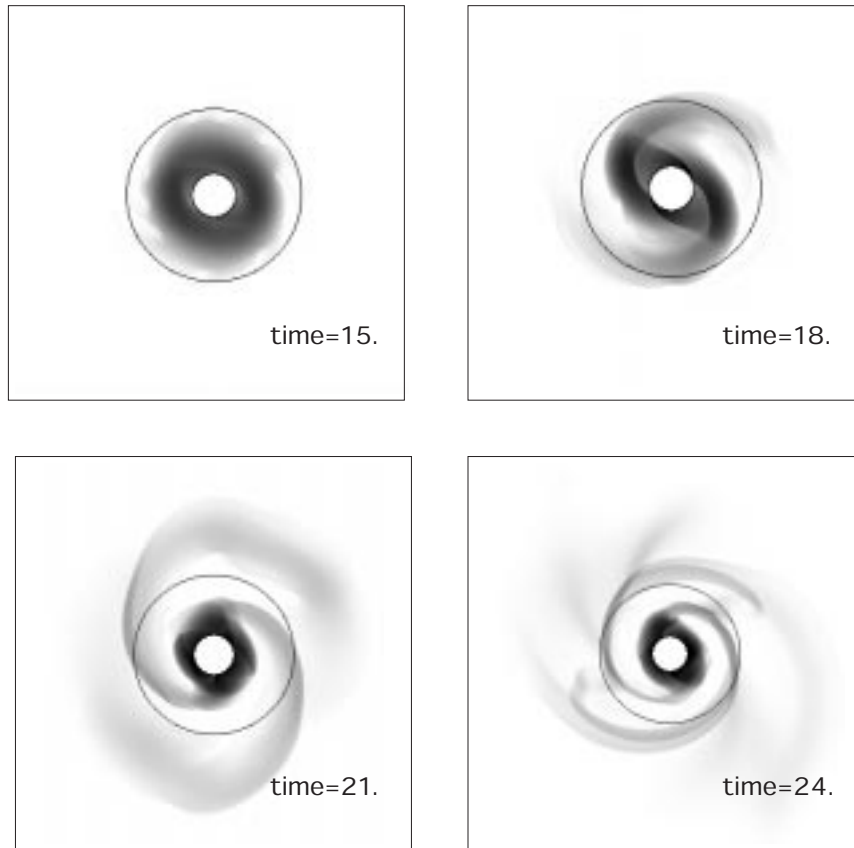
Figure 1. The surface density evolution of the model disk.

Newton's laws. Four snapshots of the resulting time evolution of the disk are shown in Fig. 1. During the time span $t = 0$–10, there is very little outward change in the disk's appearance. After t=15, the low density outer regions of the disk are slightly distorted, and there are hints of a two-armed spiral pattern. By t=18, a two-armed spiral pattern is very prominent. Soon thereafter, the strength of the spiral stabilizes, and the disk proceeds to a more or less steady state situation in which spiral fans of high angular momentum material are thrown out to large radii while the bulk of the gas in the disk creeps toward smaller radii. At the end of the simulation, the disk is distended and highly non-axisymmetric. Although the central star is allowed to move in response to gravitational forces from the material in the disk, there is very little eccentric displacement of the star during the course of the simulation.

The simulation shown in Fig. 1 has a large outer region into which disk material is allowed to freely propagate. However, if the disk is given a reflective outer boundary, its behaviour is qualitatively identical. A disk with two reflecting edges is easier to treat analytically, so we shift the discussion to a slightly more restricted disk in which both the inner and the outer boundaries are reflecting.
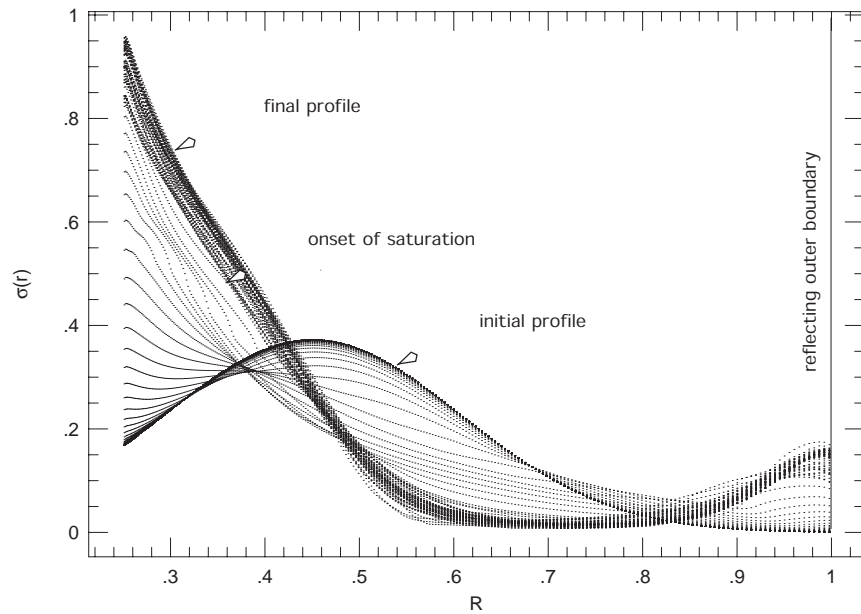
Figure 2. Evolution of the azimuthally averaged surface density profile of the model disk.

When a reflecting outer boundary is used, the material that would otherwise propagate outward in the spiral fans is compelled to pile up against the outer boundary; the time evolution of the resulting surface density profile is shown in Fig. 2. The outer pulse of material carries high specific angular momentum, and the evolutionary trend in Fig. 2 can be interpreted in light of the fact that the free energy of a rotating system with a given mass and angular momentum is minimized when the angular momentum is all in an infinitely small parcel located at infinity (Lynden-Bell and Pringle, 1974).

It has been suggested, (*e. g.*, Lin and Pringle, 1987; 1990) that the net long-term action of spiral gravitational torques on the disk gas is akin to a diffusive process which can be modeled with a so-called "alpha" type viscosity of the form: $\eta = \alpha c_s \Omega$ (Shakura and Sunyaev, 1973). This straightforward formulation has a long history of modeling diffusion arising from turbulent processes, and has proved quite robust in situations where the transport is inherently *local*. However, in self-gravitating disks of the type being considered here, the spiral instabilities are inherently *global*. As discussed by Laughlin and Różyczka (1996), a disk's α of order $\sim$0.02 can roughly model the net effective viscosity, but due to the global nature of the transport, the value of α is necessarily a function of both radius and time. In other words, describing the early evolution of the disk with an α-type model is possible, but it is also somewhat misleading. Our goal is to obtain a better overall understanding of how disks which arise in the early phases of star formation re-adjust themselves in their effort to approach an energetically favored final state.

3. The Linear Regime

At a particular radius in the disk, the "mode strength" of an m-fold azimuthal disturbance (an m armed spiral) is defined by:

$$|a_m(r,t)| = \left| \frac{1}{2\pi} \int_0^{2\pi} \sigma(r,\phi,t) e^{-im\phi} d\phi \right| . \tag{5}$$

The phase of the mode, a_m, is given by its real and imaginary parts,

$$\phi_m(r) = \tan^{-1}[\mathrm{Im}(a_m)/\mathrm{Re}(a_m)] , \tag{6}$$

and the pattern speed is given by

$$\Omega_\mathrm{P}(r) = m^{-1}[d\phi_m(r)/dt] . \tag{7}$$

The global Fourier amplitude in the disk is defined by

$$|C_m| \equiv \frac{1}{m_\mathrm{D}} \left| \int_0^{2\pi} \int_{R_\mathrm{in}}^{R_\mathrm{D}} \sigma(r,\phi) r\, dr\, e^{-im\phi} d\phi \right| . \tag{8}$$

The strength of the "$m = 0$" component is a measure of the deformation of the azimuthally averaged surface density profile away from the initial equilibrium configuration,

$$C_0 \equiv \frac{1}{m_\mathrm{D}} \int_{R_\mathrm{in}}^{R_\mathrm{D}} |(\bar{\sigma}(r) - \Sigma_0(r))| r\, dr . \tag{9}$$

Finally, the global growth rate of a mode in the disk is

$$\gamma_m = \frac{d}{dt} \ln |C_m| . \tag{10}$$

Figure 3 shows the development of the global modes ($m = 0$–4) as the hydrodynamical simulation progresses. The small random initial perturbation in every grid cell gives a baseline strength of $\log_{10} C_0 \approx -3.5$. The initial strength of the global non-axisymmetric modes is very small. By $t=7$, there is an indication that a two-armed disturbance is growing. The subsequent straight line of increase on the logarithmic plot indicates uniform exponential growth. By calculating the phase, $\phi_2(r)$, and the strength, $a_2(r)$, of the mode at a particular time ($t=11$) one can plot the appearance of the spiral mode itself, which is shown as a small inset in Fig. 3.

There is a wide literature dealing with the phenomena of exponentially growing global modes in self-gravitating disk. A detailed introduction to the problem in the context of galaxies is provided by Bertin and Lin (1996), whereas a formulation of the problem in the protostellar context is given by Adams *et al.* (1989). The particular mode which develops in our model disk is related to the "edge mode" described by Toomre (1981). The mode's existence is predicated on the declining
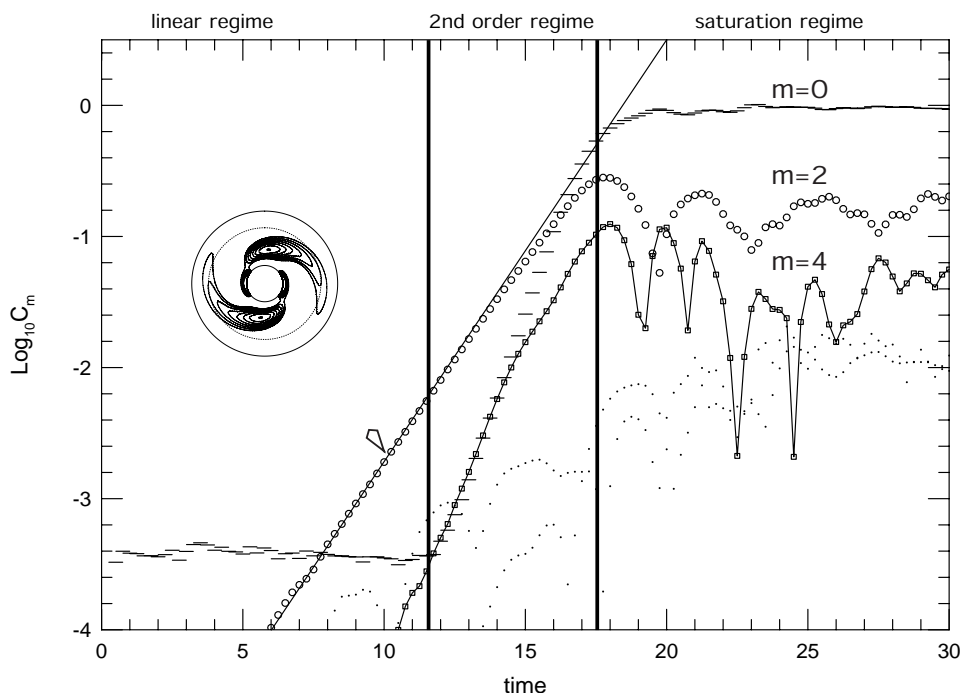
Figure 3. The development of the global amplitudes $\text{Log}_{10}|C_j|$ (for $j = 0 - 4$) during time interval t $= 0 - 30$. The m=0 components are shown as a series of horizontal bars. The linearly dominant m=2 mode is shown as open circles and the m=4 mode as connected open squares. The contributions form m=1 and m=3, which do not contribute significantly to the dynamics, are shown as small dots. The growth rate predicted by linear analysis is shown as a solid line, and the physical appearance of the dominant m=2 mode at t=11 is shown as an inset diagram.

surface density profile in the outer region of the disk, as well as on the relatively large fractional mass of the disk itself. In any case, the simulation shows quite dramatically that a chaotically stirred, differentially rotating system can spring readily into the production of a rapidly growing, yet strictly non-winding spiral pattern.

The result of the numerical simulation makes it clear that complex functions of the form:

$$\sigma(r, \phi, t) = \sigma_0(r) + \sigma_1(r) \exp[i(\omega t - m\phi)], \tag{11}$$

$$u(r, \phi, t) = u_0(r) + u_1(r) \exp[i(\omega t - m\phi)], \tag{12}$$

$$v(r, \phi, t) = v_0(r) + v_1(r) \exp[i(\omega t - m\phi)], \tag{13}$$

should provide a very good approximate solution to the hydrodynamic governing Eqs. (1–3) if σ_1, u_1, and v_1 are sufficiently small in comparison to the equilibrium values σ_0, u_0, and v_0. (Note that $\omega = m\Omega_\text{p} - i\gamma$, and that, for the disk at hand, $m = 2$, $\gamma \approx 0.7$, and $\Omega_\text{p} \approx 1.6$).

With the foreknowledge that the disk is susceptible to the exponential growth of a two-armed spiral, it is relatively straightforward to carry out a linear analysis and determine the exact properties of the mode. This done by writing down trial solutions for σ, u, v, and Ψ of the form given by Eqs. (11–13), and inserting these solutions into the momentum and continuity equations (Eqs. 1–3). Because the disturbance amplitudes f_1 are small, the nonlinear terms of the form $f_1 f_1$ will be negligible. They can be dropped. In this fashion, the equations are linearized, and after cancelling the embedded equilibrium relations, one can write:

$$(\gamma + im\Omega_p - im\Omega)\sigma_1 + \frac{1}{r}\frac{\partial}{\partial r}(r\Sigma_0 u_1) - \frac{im}{r}\Sigma_0 v_1 = 0 , \tag{14}$$

$$(\gamma + im\Omega_p - im\Omega)u_1 - 2\Omega v_1 + \frac{\partial}{\partial r}\left(\frac{c_s^2}{\Sigma_0}\sigma_1 + \Psi_1\right) = 0 , \tag{15}$$

and,

$$(\gamma + im\Omega_p - im\Omega)v_1 + \frac{\kappa^2}{2\Omega}u_1 - \frac{im}{r}\left(\frac{c_s^2}{\Sigma_0}\sigma_1 + \Psi_1\right) = 0 . \tag{16}$$

The surface density perturbation σ_1 and the potential perturbation Ψ_1 are directly related by Poisson's equation:

$$\Psi_1(r) = -2\pi G \int_{R_{\text{in}}}^{R_D} \frac{r'}{\pi r} \int_0^{\pi} \frac{\cos(m\phi)\, d\phi}{\sqrt{1 + \left(\frac{r'}{r}\right)^2 - 2\frac{r'}{r}\cos\phi + \epsilon(r)^2}}\sigma_1(r')dr' . \tag{17}$$

These are coupled, complex, first-order ordinary differential equations for σ_1, u_1, and v_1. We are assuming that the radial velocities $u(r)$ vanish at the inner and outer disk edges. To find the mode(s) endemic to a particular disk model, we also need to determine the pattern speed(s) Ω_p, and growth rate(s) γ.

One route to a mode consists of combining Eqs. (14–17) into a single integro-differential equation for the perturbed surface density σ_1, which is then solved as a matrix eigenvalue problem (*e. g.*, Pannatoni, 1979; Adams *et al.*, 1989). An alternate method, described by Noh *et al.* (1991), is to eliminate v_1 from Eqs. (14–16), leaving expressions of form (see Laughlin *et al.*, 1998)

$$\frac{d}{dr}\sigma_1(r) = F(\sigma_1(r), u_1(r), \Psi_1(r), \gamma, \Omega_p) \tag{18}$$

and

$$\frac{d}{dr}u_1(r) = G(\sigma_1(r), u_1(r), \Psi_1(r), \gamma, \Omega_p) . \tag{19}$$

These equations can be integrated using the standard techniques for ordinary differential equations. An integration proceeds by assuming (1) $u_1=0$ and an arbitrary value for σ_1 at the inner boundary, (2) guesses for the eigenvalues γ and Ω_p,
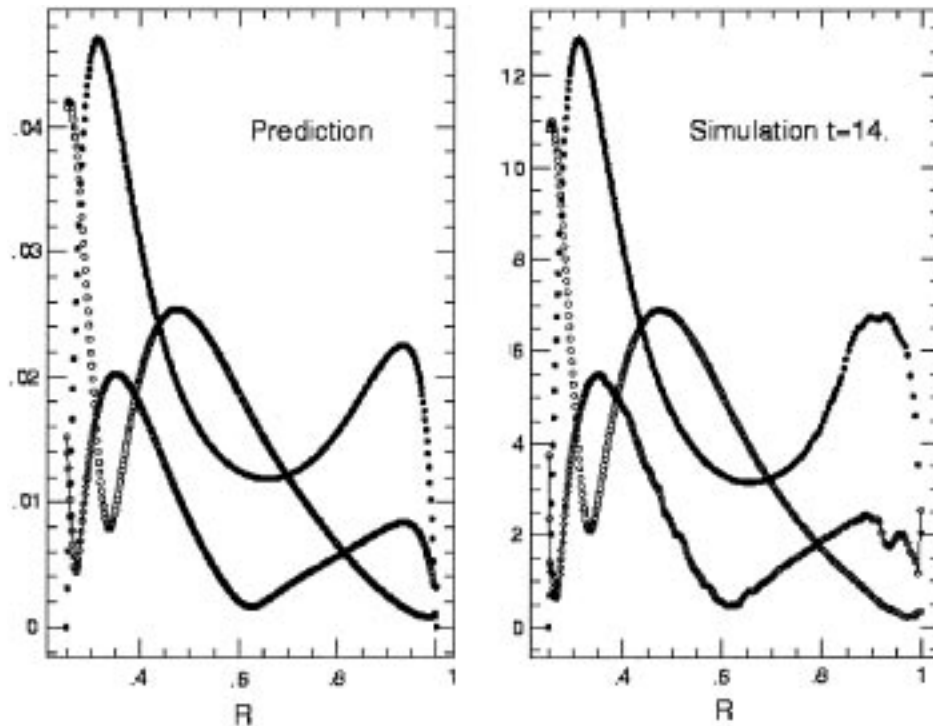
Figure 4. Comparison between the *m*=2 mode structure from the linear prediction (*left hand panel*), and the emergent mode from the nonlinear hydrodynamic simulation (*right hand panel*). Both panels depict $|\sigma_1|$ (*small open circles*), $|u_1|$ (*unconnected filled circles*), and $|v_1|$ (*connected open circles*).

and (3) a trial potential function $\Psi_1(r)$. Using a two dimensional Newton-Raphson algorithm, the eigenvalues are varied until the integration of Eq. (19) yields $u_1 = 0$ at the outer edge of the disk in accordance with the reflective boundary condition. The perturbed surface density function $\sigma_1(r)$ (obtained with the eigenvalues that yield $u_1|_{R_D} = 0$) is then used to revise the potential function $\Psi_1(r)$. This entire integration – Newton-Raphson procedure is then iterated until overall convergence is obtained. For our model disk, we find that there is a single dominant mode which has $\Omega_p = 1.71$, and $\gamma = 0.804$, in agreement with the pattern speed and the growth rate of the mode that sprang out of the simulation. In addition, we can compare the linearized solutions for σ_1, u_1, and v_1 with the spiral that emerges in the simulation. This is done in Fig. 4. The agreement is startling; linear analysis provides an excellent description of the early behaviour of the disk!

It is important to mention that our idealized model disk is rather unusual in that it happens to be susceptible to a single strongly growing two-armed mode. There is very little activity present in other linear modes. In general, a disk may have many competing modes, with similar growth rates, and this muddies the early appearance of the disk.

4. The Nonlinear Regime

A quick look at Fig. 3 shows that after $t \approx 11$, there is an upsurge of exponential growth in both a four-armed pattern and in the degree of deformation of the underlying state (the $m = 0$ component). It appears that once the $m = 2$ spiral has reached a large enough amplitude, the disk somehow responds to the rampant growth of the two-armed mode by leaking power into both the underlying flow ($m = 0$) and into the first harmonic ($m = 4$). It seems that after $t \approx 11$, the discarded nonlinear terms of form $f_1 f_1$ are no longer small enough to ignore. The disk is beginning to deform itself, and the deformation is manifest in the transport of mass and angular momentum through the disk. The next task is to obtain a better understanding of how this occurs.

In the linear analysis, we looked at the viability of solutions which behaved like rigidly rotating, exponentially growing spirals. Now we want to look for solutions which also encompass an underlying deformation of the equilibrium state of the disk. We can do this by writing the density and the velocities in the disk as the sum of perturbed and unperturbed components: $\sigma = \sigma_0 + \tilde{\sigma}$, $v = \Omega(r)r + \tilde{v}$, and $u = \tilde{u}$. These expressions are inserted into the momentum and continuity equations, and the embedded equilibrium relations are removed, leaving:

$$\left(\frac{\partial}{\partial t} + \Omega \frac{\partial}{\partial \phi}\right)\tilde{u} - 2\Omega\tilde{v} + \frac{\partial}{\partial r}\left(\tilde{\Psi} + \tilde{\Psi}_*\right) =$$

$$\frac{\tilde{v}^2}{r} - \tilde{u}\frac{\partial \tilde{u}}{\partial r} - \frac{\tilde{v}}{r}\frac{\partial \tilde{u}}{\partial \phi} - \frac{\partial}{\partial r}\left\{\frac{c_s^2}{\gamma_p - 1}\left[(1 + \tilde{\sigma}/\Sigma_0)^{\gamma_p - 1} - 1\right]\right\}, \tag{20}$$

$$\left(\frac{\partial}{\partial t} + \Omega \frac{\partial}{\partial \phi}\right)\tilde{v} + (r\Omega' + 2\Omega)\tilde{u} + \frac{1}{r}\frac{\partial}{\partial \phi}\left(\tilde{\Psi} + \tilde{\Psi}_*\right) =$$

$$-\frac{\tilde{v}\tilde{u}}{r} - \tilde{u}\frac{\partial \tilde{v}}{\partial r} - \frac{\tilde{v}}{r}\frac{\partial \tilde{v}}{\partial \phi} - \frac{1}{r}\frac{\partial}{\partial \phi}\left\{\frac{c_s^2}{\gamma_p - 1}\left[(1 + \tilde{\sigma}/\Sigma_0)^{\gamma_p - 1} - 1\right]\right\}, \tag{21}$$

and

$$\left(\frac{\partial}{\partial t} + \Omega \frac{\partial}{\partial \phi}\right)\tilde{\sigma} + \frac{1}{r}\frac{\partial}{\partial r}\left(r\Sigma_0\tilde{u}\right) + \frac{1}{r}\frac{\partial}{\partial \phi}\left(\Sigma_0\tilde{v}\right) =$$

$$-\frac{1}{r}\frac{\partial}{\partial r}\left(r\tilde{\sigma}\tilde{u}\right) - \frac{1}{r}\frac{\partial}{\partial \phi}\left(\tilde{\sigma}\tilde{v}\right). \tag{22}$$

The above equations are still fully nonlinear. We can look for solutions to Eqs. (20–22) in which the fluid fields have the particular form:

$f =$ Deformation from Equilibrium + The Known Linear Mode,

or more precisely,

$$\tilde{f} = \tilde{f}_0 + e^{\gamma t}\frac{1}{2}\left[f_1 e^{im(\Omega_p t - \phi)} + f_1^{\star} e^{-im(\Omega_p t - \phi)}\right]. \tag{23}$$

When trial solutions of this type are plugged into Eqs. (20–22), and after a lot of manipulation, one arrives at a description of the development of the axisymmetric *mode of deformation* arising from the self-interaction of the unstable $m = 2$ mode.

$$\frac{\partial \tilde{u}_0}{\partial t} - 2\Omega \tilde{v}_0 + \frac{\partial}{\partial r}\left(\frac{c_s^2}{\Sigma_0}\tilde{\sigma}_0 + \tilde{\Psi}_0\right) = NL_1(r)\,\exp[2\gamma\,t]\,, \qquad (24)$$

$$\frac{\partial \tilde{v}_0}{\partial t} + (r\Omega' + 2\Omega)\tilde{u}_0 = NL_2(r)\,\exp[2\gamma\,t]\,, \qquad (25)$$

$$\frac{\partial \tilde{\sigma}_0}{\partial t} + \frac{1}{r}\frac{\partial}{\partial r}\left(r\Sigma_0 \tilde{u}_0\right) = NL_3(r)\,\exp[2\gamma\,t]\,. \qquad (26)$$

In the above equations, the nonlinear "driving terms", $NL_1(r)$, $NL_2(r)$, and $NL_3(r)$, are complicated, but nonetheless *known* combinations of the linear eigen-functions (see Laughlin *et al.*, 1998, for a full description).

The solutions to Eqs. (24–26) describe an axisymmetric mode of deformation which grows at rate 2γ. A simple, stable method for obtaining this mode is to integrate the system of equations as an initial value problem. The resulting mod-ification of the surface density profile predicted by Eqs. (24–26) can be directly compared with the actual modification observed in the fully nonlinear numerical simulations, as shown in Fig. 5. The degree of agreement suggests that the phe-nomenon of mode self-interaction can account for the mass transport in the disk up to the moment when the $m = 0$ mode overwhelms the $m = 2$ mode. Once the background state (the $m = 0$ mode) has changed appreciably, the $m = 2$ mode is evidently unable to maintain its original growth rate, and mode saturation sets in.

It should be stressed that the computed evolution of our model disk does not rep-resent a transformation from one equilibrium state to another. In the post-saturation epoch, the disk presents a shifting kaleidoscope of non-axisymmetric spiral waves. In its attempt to reach a lower energy configuration, the system has evolved from a highly ordered axisymmetric configuration to a considerably more disordered state with many degrees of freedom.

In Laughlin *et al.* (1998), we have modelled the onset of mode saturation as arising from the stabilizing influence of the $m = 0$ mode, which in third order semi-analytic calculations, is shown to smoothly deflate the linear growth of the initially dominant two-armed spiral. Although our model disk represents a highly idealized system, we believe that rapid angular momentum and mass transport in the initial nonlinear phases may well play an important role in preventing disk fragmentation, and setting the stage for the eventual formation of single star/planetary systems.

The disk behaviour shown in Fig. 5 constitutes what may be a startling result. The rearrangement of the azimuthally averaged surface density profile represents a secular evolution of the mass distribution of the disk. It is our suspicion that this secular evolution is occurring as a result of non-linear self-interaction rather than through the offices of a dissipative mechanism such as shocks or numerical
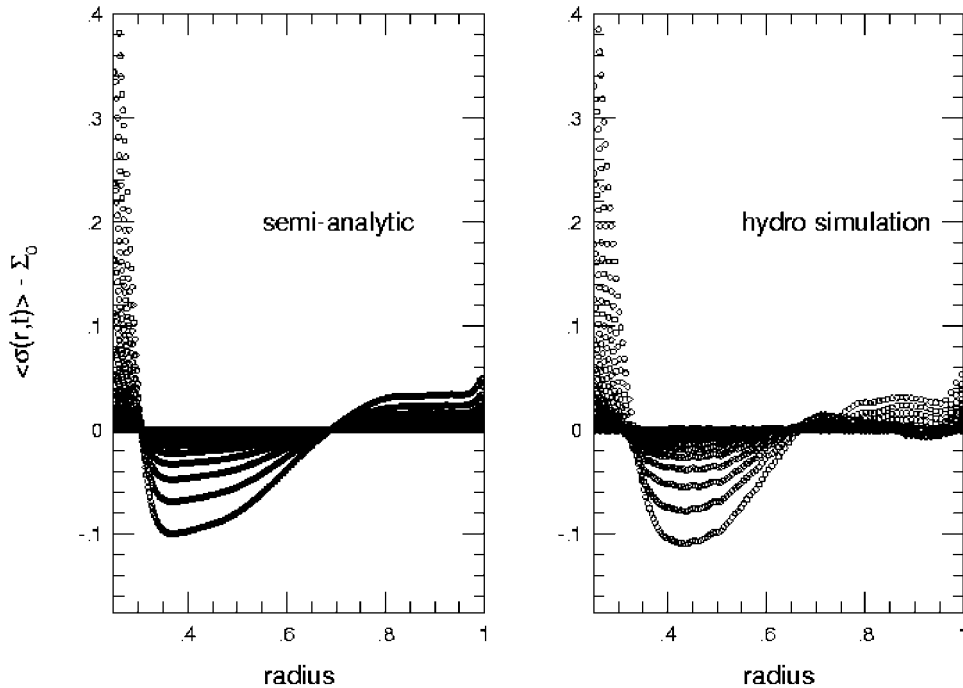
Figure 5. The development of the $m = 0$ surface density mode in the second-order nonlinear analysis (*left panel*) and in the fully nonlinear hydrodynamic simulation (*right panel*). Succesive models are spaced by equal time intervals.

dissipation. Further work must be done, however, before this conclusion can be deemed airtight. In particular, it would be interesting to perform second and third-order analyses of disks which are prone to the marginally unstable growth of tightly wound spirals. The $m = 0$ modes of deformation of such disks tend to show multiple radial zones of surface density enhancement and rarefaction (unlike the disk in Fig. 5, which has only one radial zone of rarefaction). Agreement between the semi-analytic prediction and the hydrodynamic outcome for a tightly wound spiral would further strengthen the conclusion that mode-coupling can be responsible for mass and angular momentum transport. Such calculations are now underway.

5. Conclusion

The collapse of molecular cloud cores gives rise to protostars surrounded by gaseous disks. The amount of angular momentum contained in molecular cloud cores is very significant, and it seems clear that in the very earliest phases, protostellar disks must be quite massive in comparison to the protostar. Spiral gravitational instabilities develop in massive disks, and their development has very important consequences for the ultimate fate of the system.

In particular, the saturation of gravitational instabilities has important consequences for planetary formation. If instabilities or modes can grow sufficiently nonlinear, then secondary bodies (planets and/or binary companions) can form within disks through gravity alone. If, on the other hand, modes and instabilities always saturate, then planets can be built up only through planetesimal accumulation, *i. e.*, from the bottom up. Our experience with nonlinear disk dynamics causes us to believe that mode saturation occurs quite readily as a result of mode-mode coupling. But further work is necessary to determine whether or not mode saturation always occurs before gravitational instabilities become highly nonlinear. In particular, the choice between saturation and fragmentation will require a considerably more sophisticated accounting of radiative transport than the $\gamma = 2$ polytropic simulations reported here! Future work which takes proper account of the thermal physics of the disk gas will ultimately tell us the conditions under which secondary bodies can and cannot form (through gravitational instability) in circumstellar disks.

Acknowledgements

References

Adams, F. C., and Shu, F. H.: 1986, 'Infrared Spectra of Rotating Protostars', *Astrophys. J.* **308**, 836–853.

Adams, F. C., Lada, C. J., and Shu, F. H.: 1987, 'Spectral Evolution of Young Stellar Objects', *Astrophys. J.* **312**, 788–806.

Adams, F. C., Ruden, S., and Shu, F. H.: 1989, 'Eccentric Gravitational Instabilities in Nearly Keplerian Disks', *Astrophys. J.* **347**, 959–976.

Bertin, G., and Lin, C. C.: 1996, *Spiral Structure in Galaxies, A Density Wave Theory*, MIT Press, Cambridge.

Binney, J., and Tremaine, S.: 1987, *Galactic Dynamics*, Princeton University Press, Princeton.

Bodenheimer, P.: 1995, 'Angular Momentum Evolution of Young Stars and Disks', *Annual Rev. Astron. Astrophys.* **33**, 199–238.

Boss, A. P.: 1997, 'Giant Planet Formation by Gravitational Instability', *Science* **276**, 1836–1839.

Burkert, A., Bate, M., and Bodenheimer, P.: 1997, 'Protostellar Fragmentation in a Power-Law Density Distribution', *Monthly Notices Royal Astron. Soc.* **289**, 497–504.

Butner, H. M., Evans, N. J., Lester, D. F., Levreault, R. M., and Strom, S. E.: 1991, 'Testing Models of Low-Mass Star Formation – High-Resolution Far-Infrared Observations of L1551 IRS 5', *Astrophys. J.* **376**, 636–653.

Cassen, P., and Moosman, A.: 1981, 'On the Formation of Protostellar Disks', *Icarus* **48**, 353–376.

Chevalier, R.: 1983, 'The Environments of T Tauri Stars', *Astrophys. J.* **268**, 753–765.

Galli, D., and Shu, F. H.: 1993a, 'Collapse of Magnetized Molecular Cloud Cores. I. Semianalytical Solution', *Astrophys. J.* **417**, 220–242.

Galli, D., and Shu, F. H.: 1993b, 'Collapse of Magnetized Molecular Cloud Cores. II. Numerical Results', *Astrophys. J,* **417**, 243–258.

Goodman, A., Benson, P., Fuller, G., and Myers, P.: 1993, 'Dense Cores in Dark Clouds – VIII. Velocity Gradients', *Astrophys. J.* **406**, 528–547.

Heemskerk, M. H. M., Papaloizou, J. C., and Savonije, G. J.: 1992, 'Non-Linear Development of M = 1 Instabilities in a Self-Gravitating Gaseous Disk', *Astron. Astrophys.* **260**, 161–174.

Hunter, C.: 1977, 'The Collapse of Unstable Isothermal Spheres', *Astrophys. J.*, **218**, 834–845.

Jijina, J., and Adams, F. C.: 1996, 'Infall Collapse Solutions in the Inner Limit: Radiation Pressure and Its Effects on Star Formation', *Astrophys. J.* **462**, 874–887.

Kahn, F. D.: 1974, 'Cocoons Around Early-Type Stars', *Astron. Astrophys.* **37**, 149–162.

Kenyon, S. J., Calvet, N., and Hartmann, L.: 1993, 'The Embedded Young Stars in the Taurus-Auriga Molecular Cloud – I. Models for Spectral Energy Distributions', *Astrophys. J.* **414**, 676–694.

Larson, R. B.: 1969a, *Monthly Notices Royal Astron. Soc.* **145**, 271.

Larson, R. B.: 1969b, *Monthly Notices Royal Astron. Soc.* **145**, 297.

Larson, R. B., and Starrfield, S.: 1971, 'On the Formation of Massive Stars and the Upper Limit of Stellar Masses', *Astron. Astrophys.* **13**, 190–197.

Laughlin, G.: 1994, *Ph. D. Thesis*, University of California Santa Cruz.

Lin, D. N. C., and Pringle, J. E.: 1987, 'A Viscosity Prescription for a Self-Gravitating Accretion Disk', *Monthly Notices Royal Astron. Soc.* **225**, 607–613.

Lin, D. N. C., and Pringle, J. E.: 1990, 'The Formation and Initial Evolution of Protostellar Disks', *Astrophys. J.* **358**, 515–524.

Laughlin, G., and Bodenheimer, P.: 1994, 'Nonaxisymmetric Evolution in Protostellar Disks', *Astrophys. J.* **436**, 335–354.

Laughlin, G., and Różyczka , M.: 1996, 'The Effect of Gravitational Instabilities on Protostellar Disks', *Astrophys. J.* **456**, 279–291.

Laughlin, G., Korchagin, V., and Adams, F. C.: 1997, 'Spiral Mode Saturation in Self-gravitating Disks', *Astrophys. J.* **477**, 410–423.

Laughlin, G., Korchagin, V., and Adams, F. C.: 1998, 'The Dynamics of Heavy Gaseous Disks', *Astrophys. J.* **504**, 945–966.

Lynden-Bell, D., and Pringle, J. E.: 1974, 'The Evolution of Viscous Discs and the Origin of the Nebular Variables', *Monthly Notices Royal Astron. Soc.* **168**, 603–637.

Nakano, T.: 1989, 'Conditions for the Formation of Massive Stars Through Nonspherical Accretion', *Astrophys. J.* **345**, 464–471.

Nakano, T., Hasegawa, T., and Norman, C.: 1995, 'The Mass of a Star Formed in a Cloud Core: Theory and its Application to the Orion A Cloud', *Astrophys. J.* **450**, 183–195.

Nelson, A., Benz, W., Adams, F. C., and Arnett, D.: 1998, 'Dynamics of Circumstellar Disks', *Astrophys. J.* **502**, 342–371.

Noh, H. R., Vishniac, E. T., and Cochran, W. D.: 1991, 'Gravitational Instabilities in a Proto-Planetary Disk', *Astrophys. J.* **383**, 372–379.

Pannatoni, R. F.: 1979, *Ph. D. Thesis*, Massachussettes Institute of Technology, Boston.

Shakura, N. I., and Sunyaev, R. A.: 1973, 'Black Holes in Binary Systems — Observational Appearance', *Astron. Astrophys.* **24**, 337–355.

Shu, F. H.: 1977, 'Self-Similar Collapse of Isothermal Spheres and Star Formation', *Astrophys. J.* **214**, 488–497.

Shu, F. H., Adams, F. C., and Lizano, S.: 1987, 'Star Formation in Molecular Clouds: Observation and Theory', *Ann. Rev. Astron. Astrophys.* **25**, 23–72.

Terebey, S., Shu, F. H., and Cassen, P.: 1984, 'The Collapse of the Cores of Slowly Rotating Isothermal Clouds', *Astrophys. J.* **286**, 529–551.

Tomley, L., Steiman-Cameron, T. Y., and Cassen, P.: 1994, 'Further Studies of Gravitationally Unstable Protostellar Disks', *Astrophys. J.* **422**, 850–861.

Toomre, A.: 1981, 'What Amplifies the Spirals', *in* S. M. Fall and D. Lynden-Bell (eds.), *The Structure and Evolution of Normal Galaxies*, Cambridge Univ. Press, Cambridge, pp. 111–136.

Ulrich, R. K.: 1976, 'An Infall Model for the T Tauri Phenomenon', *Astrophys. J.* **210**, 377–391.

Wolfire, M. G., and Cassinelli, J.: 1986, 'The Temperature Structure in Accretion Flows Onto Massive Protostars', *Astrophys. J.* **310**, 207–221.

Wolfire, M. G., and Cassinelli, J.: 1987, 'Conditions for the Formation of Massive Stars', *Astrophys. J.* **319**, 850–867.

Woodward, J. W., Tohline, J. E., and Hachisu, I.: 1994, 'The Stability of Thick, Self-Gravitating Disks in Protostellar Systems', *Astrophys. J.* **420**, 247–267.

Yorke, H. W., Bodenheimer, P., and Laughlin, G.: 1993, 'The Formation of Protostellar Disks. I. 1 $M_\odot$', *Astrophys. J.* **411**, 274–284.

Address for Offprints: Gregory Laughlin, NASA Ames Research Center, Moffett Field, CA 94720